

Copyright  
by  
Tianyang Bai  
2013

The Thesis committee for Tianyang Bai

Certifies that this is the approved version of the following thesis

**Analysis of Blockage Effects on Urban Cellular  
Networks**

APPROVED BY

SUPERVISING COMMITTEE:

---

Robert W. Heath, Jr., Supervisor

---

François Baccelli

**Analysis of Blockage Effects on Urban Cellular  
Networks**

by

**Tianyang Bai, B.E.**

**THESIS**

Presented to the Faculty of the Graduate School of  
The University of Texas at Austin  
in Partial Fulfillment  
of the Requirements  
for the Degree of

**MASTER OF SCIENCE IN ENGINEERING**

THE UNIVERSITY OF TEXAS AT AUSTIN

May 2013

Dedicated to my parents, Hong Huo and Dr. Shizhen Bai.

## Acknowledgments

I would like to start by thanking my parents for their support through my education. All my academic success can be traced back to them. I would like to thank my advisor Prof. Robert Heath for serving as a mentor during my graduate studies, and the role model of my career. Dr. Heath gave me many insightful suggestions, which were fundamental to my accomplishments. I am grateful to my committee member Prof. François Baccelli for his comments, insights, and more importantly, his great instructions on stochastic geometry. I would also like to thank all my friends, who provide enough laughs and entertainment in my life.

# Analysis of Blockage Effects on Urban Cellular Networks

by

Tianyang Bai, M.S.E.

The University of Texas at Austin, 2013

Supervisor: Robert W. Heath, Jr.

Large-scale blockages like buildings affect the performance of urban cellular networks, especially in the millimeter-wave frequency band. Unfortunately, such blockage effects are either neglected or characterized by oversimplified models in the analysis of cellular networks. Leveraging concepts from random shape theory, this paper proposes a mathematical framework to model random blockages, and quantifies their effects on the performance of cellular networks. Specifically, random buildings are modeled as a process of rectangles with random sizes and orientations whose centers form a Poisson point process on the plane, which is called a Boolean scheme. The distribution of the number of blockages in a link is proven to be Poisson with parameter dependent on the length of the link, which leads to the distribution of penetration losses of a single link. A path loss model that incorporates the blockage effects is proposed, which matches experimental trends observed in prior work. The blockage model is applied to analyze blockage effects on cellular networks

assuming blockages are impenetrable, in terms of connectivity, coverage probability, and average rate. Analytic results show while buildings may block the desired signal, they may still have a positive impact on network performance since they also block more interference.

# Table of Contents

<b>Acknowledgments</b>	<b>v</b>
<b>Abstract</b>	<b>vi</b>
<b>List of Tables</b>	<b>x</b>
<b>List of Figures</b>	<b>xi</b>
<b>Chapter 1. Introduction</b>	<b>1</b>
<b>Chapter 2. System Model</b>	<b>7</b>
2.1 Background on Random Shape Theory . . . . .	7
2.2 Cellular Network Model with Random Buildings . . . . .	10
<b>Chapter 3. Quantification of Blockage Effects</b>	<b>14</b>
3.1 Distribution of the Number of Blockages . . . . .	15
3.2 Incorporating Height . . . . .	20
3.3 Quantification of Power Losses by Blockages . . . . .	23
3.4 Analysis of Blockage Effects on Link Budget . . . . .	28
<b>Chapter 4. Analysis of Blockage effects on Impenetrable Networks</b>	<b>31</b>
4.1 Connectivity . . . . .	32
4.2 Coverage Probability . . . . .	38
4.3 Average Achievable Rate . . . . .	41
<b>Chapter 5. Simulation Results</b>	<b>43</b>
<b>Chapter 6. Conclusion</b>	<b>49</b>
<b>Bibliography</b>	<b>51</b>





## List of Tables

5.1	Average Rate Comparison With $M = 10dB$ . . . . .	47
-----	---	----

## List of Figures

3.1	Proof of Lemma 3.1.2 . . . . .	18
3.2	Proof of Theorem 3.2.1 . . . . .	21
5.1	Comparison between the Boolean scheme model and lattice model in terms of coverage probability . . . . .	44
5.2	Blockage effects on network connectivity . . . . .	45
5.3	Comparison between analytic results of coverage probability and Monte Carlo simulations . . . . .	46
5.4	Coverage probability in impenetrable networks with different blockage densities . . . . .	48

# Chapter 1

## Introduction

Penetration losses due to densely located buildings make it hard to predict coverage of cellular networks in urban areas. Such blockage effects become more severe with systems of higher frequencies, and may limit performance, such as in millimeter-wave cellular networks [1, 2]. Blockages impact system functions like user association and mobility. For instance, a mobile user may associate with a farther base station with line-of-sight transmission rather than a closer base station that is blocked. Traditionally, blockage effects are incorporated into the shadowing model, along with reflections, scattering, and diffractions of signals [3]. Shadowing of different links is often modeled by using a log-normal distributed random variables, with the variance determined from measurements. Unfortunately, this approach does not capture the distance-dependence of blockage effects: intuitively speaking, the longer the link, the more buildings are likely to intersect it, hence more shadowing is likely to be experienced.

Cellular networks are becoming less regular as a variety of demand-based low power nodes is being deployed [4]. Moreover, as urban areas are built out, even the locations of the macro and micro base stations are becoming

random and less like points in a hexagonal grid [5]. Fortunately, mathematical tools like stochastic geometry make it possible to analyze cellular networks with randomly located infrastructure [5–9]. With stochastic geometry, the locations of the infrastructure are often assumed to be distributed according to a spatial point process, usually a homogenous Poisson point process (PPP) for tractability. In [6], a shotgun cellular system in which base stations are distributed as a PPP was shown to lower bound a hexagonal system in terms of certain performance metrics. In [5], a tractable approach was proposed to compute average performance metrics, such as the coverage probability and the average rate, of a cellular network with PPP distributed base stations. In [8, 10] the results were extended to multi-tier networks. In a recent work of [9], a hybrid model in which only interferers are modeled as a PPP outside a fixed-size cell was proposed to characterize the site-specific performance of cells with different sizes, rather than the aggregate performance metrics of the entire system. Blockages due to buildings in urban areas were not explicitly incorporated. Blockage effects were either neglected for simplicity or incorporated into a log-normal shadowing random variable.

There are two popular approaches that elaborately take into account the effects of blockages on wireless propagation. One approach is using ray tracing to employ site-specific simulations [11, 12]. Ray tracing requires accurate terrain information, such as the location and size of the blockages in the network to generate the received signal strength given a base station deployment. Ray tracing trades the complexity of numerical computation for an

accurate site-specific solution. The second approach is to establish a stochastic model to characterize the statistics of blockages that provides acceptable estimation of the blockage effects with only a few parameters. One advantage of stochastic models is that it may be possible to analyze general networks. In [13–15], urban areas were modeled as random lattices, which are made up of sites of unit squares. Each site is occupied by a blockage with some probability. It was assumed that signals reflect when impinging blockages with no power losses. The methods from percolation theory were applied to derive a closed-form expression of the propagation depth into the random lattice. The study did not take penetration losses of signals into account. Moreover, its application is better suited for regular Manhattan-type cities where all blockages on the plane have the similar size and orientation. In [16], the lattice model from [13] was extended by removing some of the restrictions. A constant power loss of signal is assumed when it impinges at the blockages. Orientation of blockages are also randomly distributed. Such refinements are achieved by representing blockages as nuclei from a point process, where the difference of the sizes of the blockages was not explicitly incorporated. In addition, one common limitation of the prior work is that the factor of heights is ignored by restricting the model to the plane of  $\mathbb{R}^2$ . The models in [13–15] are not compatible with stochastic geometry network model that provides a convenient analysis of cellular networks [5].

In this work, the concept of the *Boolean scheme* (also called as Boolean model) from stochastic geometry is applied to model the random blockages in

a tractable manner. The initial research on the Boolean scheme was mainly performed by the Fontainebleau school [17], e.g. see [18]. Fortunately, many quantitative properties of the Boolean scheme model, such as the covering and connectivity properties have been investigated in a general mathematical framework [19]. We will apply these general results to analyze the blockage effects on network performance in the following chapters. Besides, the concept of the Boolean scheme is also used in other interesting topics of wireless networks, such as network percolation [20].

The main contribution of this thesis is to propose a mathematical framework to model blockages with random sizes, locations, and orientations in cellular networks using concepts from random shape theory. We remove the restrictions on the orientations and sizes of the blockages as in the prior lattice models. Specifically, random buildings in urban area are modeled as a Boolean scheme of rectangles with random sizes and orientations whose centers form a PPP, which is more general than the line segment process we used previously in [21]. We also extend the blockage model to incorporate the factor of height. The proposed framework applies to the general case with blockages of arbitrary shapes. It is also convenient to combine the proposed blockage model with the PPP cellular network model, which leads to tractable analysis of the network performance. Based on the proposed model, we derive the distribution of power losses due to blockages in a link, and apply it to analyze the performance of cellular networks with impenetrable blockages. Analytical results indicate that while buildings complicate the environment of wireless

propagation by blocking line-of-sight links, they improve system performance in covered area by blocking more interference. Compared with our prior work in [21], in this paper we provide a general mathematical framework to model random blockages, and evaluate the network performance with blockages more precisely, which is based on the distribution rather than the moments of interference.

The main limitation of our work is that we only consider the direct propagation path, and ignore the reflections of signals, which is an important component of wireless transmissions. The assumption might be a good approximation in the millimeter-wave cellular network, where reflections are weak due to the high carrier frequency, and signals are highly directive with the deployment of adaptive antenna arrays at both transmitters and receivers [1]. We also assume independence of links in terms of blockage effects when analyzing network performance, which neglects correlation induced by large buildings. Simulation results show that the error of such approximation is minor and acceptable.

The thesis is organized as follows. In the next chapter, after briefly reviewing the concepts from random shape theory, we describe the system model where blockages are modeled as a random process of rectangles. In Chapter 3, we derive the distribution of blockage number on a link, and apply it to quantify penetration losses of a link. We also extend results to incorporate the height of blockage. In Chapter 4, we analyze blockage effects on a specific case of cellular networks in which blockages are impenetrable to signals, in terms of



coverage probability, average achievable rate, and network connectivity. Simulation results and comparison with the prior lattice model are provided in Chapter 5. Conclusions are drawn in Chapter 6.

**Notation:** We use the following notation throughout this paper: bold letters  $\mathbf{a}, \mathbf{A}$  are used to denote vector, non-bold letters  $a, A$  are used to denote scalar values, and caligraphic letters  $\mathcal{A}$  used to denote sets. Using this notation,  $|\mathbf{A}|$  is the  $\ell - 2$  norm of a vector,  $V(\mathcal{A})$  is the volume of a set in  $n$ -dimensional Euclidean space  $\mathbb{R}^n$ . We denote the origin of  $\mathbb{R}^n$  as  $\mathbf{O}$ . We use  $\mathbb{E}$  to denote expectation, and  $\mathbb{P}$  to denote probability.

# Chapter 2

## System Model

In this chapter, we propose a system model for urban cellular networks that incorporates random blockages like buildings. To fully characterize the random nature of the blockages in terms of sizes, orientations and locations, we apply concepts from random shape theory to model the blockages. Random shape theory is a branch of advanced geometry that formalizes random objects in space. We use random shape theory to model buildings as a process of random rectangles while base stations are distributed according to a PPP. In this section, we review concepts from random shape theory. Then based on several mathematical assumptions, we describe the system mode.

### 2.1 Background on Random Shape Theory

Random shape theory is a branch of stochastic geometry that deals with random distributions of shapes in space [22, 23]. In this section, we will explain the concepts for  $\mathbb{R}^n$ . However, in this paper we focus on the case where objects lie in the  $\mathbb{R}^2$  plane. We will regard the height of blockages as independent marks associated with the objects.

Let  $\mathcal{S}$  be a set of bounded objects which are closed, bounded, with

finite area and perimeter in  $\mathbb{R}^n$  space. For example,  $\mathcal{S}$  could be a collection of balls with different volumes in  $\mathbb{R}^3$  space, or a combination of line segments, rectangles, ellipses on  $\mathbb{R}^2$  space. For each element  $s \in \mathcal{S}$ , a point is defined to be its *center*. The center here does not necessarily to be the geographic center of the object: any well defined point will suffice. When an object is not symmetric in the space, it is also necessary to define the orientation of the object. The orientation is characterized by a directional unit vector originating from its center.

The concept of random object process will be used throughout the paper. A random object process (ROP) is constructed in the following way. First randomly sample objects from  $\mathcal{S}$  and place the centers of these objects in  $\mathbb{R}^n$  at points generated by a point process  $\mathcal{P}$ . Second, determine the orientation of each object according to some distribution.

For instance, to establish a random object process of line segments on  $\mathbb{R}^2$  plane, first we sample segments from  $\mathcal{S}$ , namely decide the lengths of the segments. Second we determine the angle between the directional vector of each line segment and the  $x$ -axis according to some distribution ranging on  $[0, 2\pi)$ .

In general cases, a random object process is complicated, especially when correlations exist between objects or between the sampling, location, orientation of an object. In this paper, we focus on a special class of object processes known as Boolean scheme, which satisfies the following properties.

- The center points form a PPP.
- For all objects  $s \in \mathcal{S}$ , the attributes of an object, e.g. orientation, shape, and volume, are mutually independent.
- For a specific object, its sampling, location, and orientation are also independently.

Note that the PPP property of the centers guarantees that the locations of different objects are independent. Hence it can be concluded that the attribute of objects, such as the size, location, and orientation, are independent in Boolean schemes. Such assumptions of independence provide much tractability in the analysis of network model.

The operation of Minkowski sum (also known as dilation) is often used in the context of stochastic geometry. In Euclidean space, the Minkowski sum is defined as follows.

**Definition 2.1.1.** The Minkowski sum of two compact sets  $\mathcal{A}$  and  $\mathcal{B}$  in  $\mathbb{R}^n$  is

$$\mathcal{A} \oplus \mathcal{B} = \cup_{\mathbf{x} \in \mathcal{A}, \mathbf{y} \in \mathcal{B}} (\mathbf{x} + \mathbf{y}). \quad (2.1)$$

Note that for any compact set  $\mathcal{A}$  and  $\mathcal{B}$  in  $\mathbb{R}^n$ , the volume of their Minkowski sum  $V(\mathcal{A} \oplus \mathcal{B})$  is finite. The concept of Minkowski sum enables us to generate results obtained in a special case to general cases in the following sections.

## 2.2 Cellular Network Model with Random Buildings

We describe the system model of cellular networks with random blockages leveraging concepts from random shape theory. We use Boolean schemes of random rectangles to model random buildings. Note that the rectangle process is more general than the line segment process we used in [21], for line segments can be viewed as a special kind of rectangles whose widths are zero.

We focus on the network with a single tier of base stations. The cellular network model is established with the following assumptions.

**Assumption 2.2.1** (PPP Base Station). *The locations of the base stations are assumed to form a homogenous PPP  $\{\mathbf{X}_i\}$  on the  $\mathbb{R}^2$  plane with density  $\mu$ . A fixed transmission power  $P_t$  is assumed for each base station. A typical user, located at the origin, will be used for the analysis of performance. Denote the link from base station  $X_i$  to the typical user as  $\mathbf{OX}_i$ , and  $|\mathbf{OX}_i| = R_i$ .*

**Assumption 2.2.2** (Boolean Scheme Blockages). *Blockages, such as buildings, are assumed to form a Boolean scheme of rectangles. Namely, the centers of the rectangles  $\{\mathbf{C}_k\}$  form a homogenous PPP of density  $\lambda$ . We further assume that the lengths  $L_k$  and widths  $W_k$  of all rectangles are i.i.d. distributed according to some probability density function  $f_L(x)$  and  $f_W(x)$  respectively. The orientation of the rectangles  $\Theta_k$  is assumed to be uniformly distributed in  $(0, 2\pi]$ .*

Note that by Assumption 2.2.2, for any fixed index  $k$ ,  $L_k$ ,  $W_k$ , and  $\Theta_k$  are independent. If  $W \equiv 0$ , the rectangle process degenerates to the line

segment process. The Boolean scheme of blockages is completely characterized by the quadruple  $\{\mathbf{C}_k, L_k, W_k, \Theta_k\}$  as the object set of the buildings is defined by  $\{L_k, W_k, \Theta_k\}$ . Moreover, we define a location  $\mathbf{x}$  in  $\mathbb{R}^2$  is indoor or contained by a blockage if and only if there exists an index  $k$ , such that  $\mathbf{x} \in D_k$ , where  $D_k$  is the rectangle blockage centered at  $\mathbf{C}_k$ .

**Assumption 2.2.3** (Independent Height). *Assume i.i.d. height for each blockage. Denote  $H_k$  as the height of the  $k$ -th blockage. let the probability density function of  $H_k$  be  $f_H(x)$ .*

In Section 3.1, as the first step of analysis, we will ignore the factor of heights by restricting our model in  $\mathbb{R}^2$  space. However, we will extend the results to incorporate height in Section 3.2.

**Assumption 2.2.4** (No Reflections). *Ignore the reflections of signals on the surface of the blockages, i.e consider only the direct propagation of signals in this paper.*

Discussions on the reflection paths due to blockages can be found in [14, 15]. However, we defer the incorporation of the reflection paths for future work.

**Assumption 2.2.5** (Rayleigh fading, No Noise). *Assume i.i.d. small-scale Rayleigh fading in each link. Assume the network is interference-limited, i.e. ignore thermal noise in analysis.*

Let  $P_i$  be the received power by the mobile user from base station  $\mathbf{X}_i$ . Based on our assumptions above,  $P_i$  can be expressed as

$$P_i = \frac{Mg_i \prod_{k=0}^{K_i} \gamma_{ik}}{R_i^\alpha}, \quad (2.2)$$

where  $M$  is a constant mainly determined by the signal frequency, antenna gains, and the transmitted power  $P_t$ ;  $g_i$  is an exponential random variable of mean 1 accounting for small-scale fading;  $\alpha$  is the exponent of path loss, which is normally between 2 and 4;  $K_i$  is the number of buildings on the link  $\mathbf{O}\mathbf{X}_i$ ;  $\gamma_{ik}$  is the ratio of penetration power losses caused by the  $k$ -th ( $0 < k < K_i$ ) blockage on  $\mathbf{O}\mathbf{X}_i$ , which takes value on  $[0, 1]$ , for the blockages attenuate signal power when ignoring reflections. Note that  $\prod_{k=0}^{K_i} \gamma_{ik}$  is the penetration loss of power caused by blockages, which we aim to quantify in this paper.

In one special case, if all buildings in the networks have the same ratio of power losses, i.e.  $\forall i, k, \gamma_{ik} = \gamma$ , then (2.2) can be written as

$$P_i = \frac{Mg_i \gamma^{K_i}}{R_i^\alpha}. \quad (2.3)$$

If all buildings are impenetrable, then  $\forall i, k, \gamma_{ik} = 0$ . The *impenetrable* case is a good approximation especially when the frequency of the signals becomes higher such as in the millimeter communication networks, for signals of higher frequency suffer from severer penetration losses through many solid materials [16].

With  $\gamma_{ik} = \gamma$ , the signal-to-interference ratio when the mobile user is served by base station  $\mathbf{X}_i$  can be written as

$$\text{SIR}(\mathbf{X}_i) = \frac{g_i \gamma^{K_i} R_i^{-\alpha}}{\sum_{\ell: \ell \neq i} h_\ell \gamma^{K_\ell} R_\ell^{-\alpha}} \quad (2.4)$$



## Chapter 3

### Quantification of Blockage Effects

In this chapter, we quantify the power losses due to blockages on a given link  $\mathbf{OX}_i$  in the cellular networks. Namely, based on the system model, we would like to derive the distribution of  $S_i = \prod_{k=0}^{K_i} \gamma_{ik}$ , the ratio of power losses due to blockages on  $\mathbf{OX}_i$ . Towards that end, the distribution of the blockage number  $K_i$  is investigated in  $\mathbb{R}^2$ , and generalized to incorporate height thereafter. Then we introduce a systematic method to calculate the distribution of  $S_i$  in general cases using Laplace transform. As the distribution of  $S_i$  is difficult to obtain in closed form, we further approximate it using a beta distribution by matching the moments. Last we analyze the effect of blockage on the link budget of a single link. We show that blockages on average introduce an additional exponential decay term into the path loss formula, which also matches the results from field experiments in prior work [15]. Since we focus on the blockage effects on a single link  $\mathbf{OX}_i$ , the subscript  $i$ , which is the index for links, will be omitted in this section without causing any confusion.

### 3.1 Distribution of the Number of Blockages

To quantify the effect of penetration losses, the distribution of the blockage number  $K$  is required. Discussions on counting the number of components of a general Boolean model, which intersect a specific set can be found in [19, 23] under a general mathematical framework. In this section, we derive the distribution of  $K$  in a concrete case of a rectangle Boolean model in  $\mathbb{R}^2$  using some elementary properties of PPP.

We denote the point process which is formed by centers of the rectangles with lengths in  $(\ell, \ell + d\ell)$ , widths in  $(w, w + dw)$ , and orientations in  $(\theta, \theta + d\theta)$  as  $\Phi(\ell, w, \theta)$ . Note that  $\Phi(\ell, w, \theta)$  is a subset (partition) of the center point process  $\{C_k\}$ , and is a PPP according to the following lemma.

**Lemma 3.1.1.**  *$\Phi(\ell, w, \theta)$  is a PPP with the density*

$$\lambda_{\ell, w, \theta} = \lambda f_L(\ell) d\ell f_W(w) dw f_\Theta(\theta) d\theta.$$

*If  $(\ell_1, w_1, \theta_1) \neq (\ell_2, w_2, \theta_2)$ , then  $\Phi(\ell_1, w_1, \theta_1)$  and  $\Phi(\ell_2, w_2, \theta_2)$  are independent processes.*

*Proof.* By the definition of Boolean scheme,  $\{C_k\}$  is a PPP, and  $\{L_k\}$ ,  $\{W_k\}$ , and  $\{\Theta_k\}$  are sequences of i.i.d. random variables. Since the Poisson law is preserved by the operation of independent thinning [20],  $\Phi(\ell, w, \theta)$  is a PPP. Moreover, processes obtained from different thinning conditions form independent PPPs. □

Next we focus on investigating a particular subset of the blockages.

Define the subset as

$$\mathcal{B}(\ell, w, \theta) = \{(C_k, L_k, W_k, \Theta_k), C_k \in \Phi(\ell, w, \theta)\},$$

which is the collection of blockages with lengths  $(\ell, \ell + d\ell)$ , widths  $(w, w + dw)$ , and orientations  $(\theta, \theta + d\theta)$ . Denote the number of blockages, which belong to  $\mathcal{B}(\ell, w, \theta)$  and cross the link  $\mathbf{OX}$ , as  $K(\ell, w, \theta)$ . We derive the distribution of  $K(\ell, w, \theta)$  in Lemma 3.1.2.

**Lemma 3.1.2.**  *$K(\ell, w, \theta)$ , the number of rectangles in  $\mathcal{B}(\ell, w, \theta)$  which cross the link  $\mathbf{OX}$  of length  $R$ , is a Poisson random variable with mean*

$$\mathbb{E}[K(\ell, w, \theta)] = \lambda_{\ell, w, \theta}(R\ell|\sin\theta| + Rw|\cos\theta| + \ell w).$$

*Proof.* As shown in Fig. 3.1, a rectangle of  $\mathcal{B}(\ell, w, \theta)$  intersects the link  $\mathbf{OX}$  if only if its center falls in the region  $PQRSTUV$ . Let the area of region  $PQRSTUV$  be  $S(\ell, w, \theta)$ , then

$$\begin{aligned} S(\ell, w, \theta) &= R|\sin(\phi + \theta)|\sqrt{w^2 + \ell^2} + \ell w \\ &= R\left(|\sin(\theta)|\frac{\ell}{\sqrt{w^2 + \ell^2}} + |\cos(\theta)|\frac{w}{\sqrt{w^2 + \ell^2}}\right)\sqrt{w^2 + \ell^2} + \ell w \\ &= R\ell|\sin\theta| + Rw|\cos\theta| + \ell w. \end{aligned}$$

Recall that  $\Phi(\ell, w, \theta)$  is the point process formed by centers of rectangles belonging to  $\mathcal{B}(\ell, w, \theta)$ . By Lemma 3.1.1  $\Phi(\ell, w, \theta)$  is a PPP of density  $\lambda_{\ell, w, \theta}$ . Hence  $K(\ell, w, \theta)$ , the number of rectangles of  $\mathcal{B}(\ell, w, \theta)$  intersecting  $\mathbf{OX}$  equals

the number of points of  $\Phi(\ell, w, \theta)$  falling in the region  $PQSTUV$ , which completes the proof as

$$\begin{aligned}\mathbb{E}[K(\ell, w, \theta)] &= \lambda_{\ell, w, \theta} S(\ell, w, \theta) \\ &= \lambda_{\ell, w, \theta} \times (R\ell |\sin \theta| + R w |\cos \theta| + \ell w).\end{aligned}$$

□

*Remark 3.1.1.* Note the fact that

$$S(\ell, w, \theta) = V(OX \oplus D_{\ell, w, \theta}),$$

where  $\oplus$  is the Minkowski sum as defined earlier, and  $D_{\ell, w, \theta}$  is a typical element of  $\mathcal{B}(\ell, w, \theta)$ , i.e a rectangle of length  $\ell$ , width  $w$ , and orientation  $\theta$ .

Hence  $\mathbb{E}[K(\ell, w, \theta)]$  can be also expressed as

$$\mathbb{E}[K(\ell, w, \theta)] = \lambda_{\ell, w, \theta} \times V(\mathbf{OX} \oplus D_{\ell, w, \theta}). \quad (3.1)$$

Next we further obtain the distribution of the total number of blockages crossing a link in the following theorem.

**Theorem 3.1.1.** *The number of blockages crossing a link of length  $R$ ,  $K$  is a Poisson random variable with the mean  $\beta R + p$ , where  $\beta = \frac{2\lambda(\mathbb{E}[W] + \mathbb{E}[L])}{\pi}$ , and  $p = \lambda\mathbb{E}[L]\mathbb{E}[W]$ .*

*Proof.* By Lemma 3.1.1 and Lemma 3.1.2,  $K(\ell, w, \theta)$  are independent Poisson random variables for different values of the tuple  $(\ell, w, \theta)$ . Note that for any realization of blockage distribution,  $K = \sum_{\ell, w, \theta} K(\ell, w, \theta)$  always hold. Since

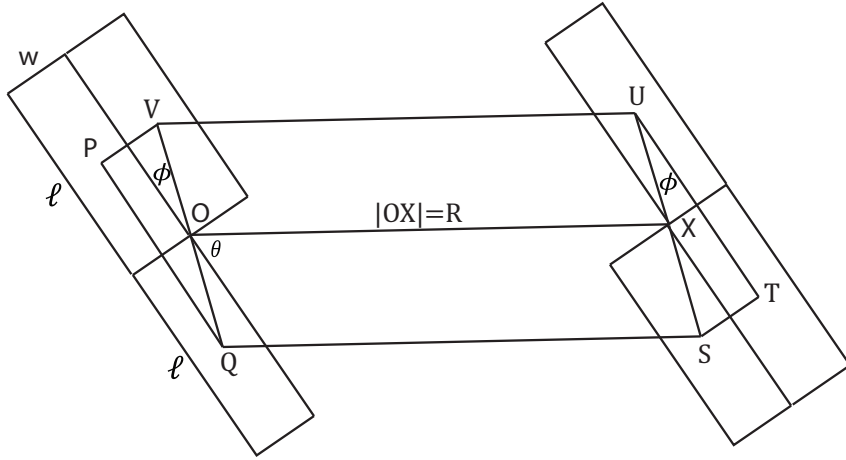


Figure 3.1:  $OX$  is the link of distance  $R$ .  $P, Q, S, T, U$ , and  $V$  are the centers of the corresponding rectangles. A rectangle of  $B(\ell, w, \theta)$  intersects  $OX$  if only if its center falls in the region  $PQSTUV$ , which is made up of parallelogram  $QSU$  and right triangles  $PQV$  and  $TSU$ .

superpositions of independent Poisson variables are still Poisson,  $K$  is Poisson distributed. Its expectation can be computed as

$$\begin{aligned}
\mathbb{E}[K] &= \sum_{\ell, w, \theta} K(\ell, w, \theta) \\
&= \int_L \int_W \int_{\Theta} \lambda (R\ell |\sin \theta| + Rw |\cos \theta| + \ell w) f_L(\ell) d\ell f_W(w) dw \frac{1}{2\pi} d\theta \\
&= \frac{2\lambda(\mathbb{E}[L] + \mathbb{E}[W])}{\pi} R + \lambda \mathbb{E}[L] \mathbb{E}[W] \\
&= \beta R + p.
\end{aligned}$$

□

According to Theorem 3.1.1, the average number of blockages on a link is proportional to the length of the link, which matches the intuition that

the longer the link is, the more blockages are likely to appear on that link. Also, when  $W \equiv 0$ , i.e using line segments instead of rectangles to describe blockages,  $\mathbb{E}[K] = \frac{2\lambda\mathbb{E}[L]R}{\pi}$ , which matches our previous results in [21].

The probability of line-of-sight propagation through a link can be evaluated through the following corollary.

**Corollary 3.1.1.1.** *The probability that a link of length  $R$  admits line-of-sight propagation, i.e no blockages cross the link, is  $\mathbb{P}(K = 0) = e^{-(\beta R + p)}$ .*

We can also evaluate the probability that a user is located inside a building in the following lemma.

**Corollary 3.1.1.2.** *The probability that a location on the plane is contained by a blockage is  $1 - e^{-p} \approx p$*

*Proof.* This follows immediately from Corollary 3.1.1.1 by taking  $R = 0$ . The approximation is based on the fact that  $\lim_{p \rightarrow 0} \frac{1 - e^{-p}}{p} = 1$ .  $\square$

Therefore,  $p$  is an approximation of the fraction of the land covered by blockages in the investigated area. The error of approximation is caused by neglecting the overlapping of blockages, which does exist in the Boolean scheme model. If buildings are not allowed to overlap,  $p = \lambda\mathbb{E}[L]\mathbb{E}[W]$  becomes the exact evaluation of blockage coverage. Intuitively speaking, with small  $p$ , which indicates the blockages are sparsely distributed, blockages are unlikely to overlap. Therefore in this case the error due to overlap is negligible. This

provides a method to determine the parameters of our blockage model in practice. Besides,  $p$  is defined as the volumn fraction in the general mathematical framework of stochastic geometry, and can be evaluated through computing the capacity functional of the Boolean model [17].

*Remark 3.1.2.* The average number of blockages  $\mathbb{E}[K]$  can be also rewritten using Minkowski addition as

$$\mathbb{E}[K] = \lambda \mathbb{E}[V(\mathbf{OX} \oplus D)], \quad (3.2)$$

where  $D$  is an element of the object set of the Boolean scheme, and the expectation operation on the right hand side is taken over the object set  $\{L_k, W_k, \Theta_k\}$ .

The results in Theorem 3.1.1 are extended to the general case in which the objects can be any compact set in  $\mathbb{R}^2$  as the following theorem. The proof is similar to that of Theorem 3.1.1, and is omitted. The result is also a special case of the general results derived in stochastic geometry, which can be found in [24].

**Theorem 3.1.2.** *Assume the blockages form a Boolean scheme in  $\mathbb{R}^2$  space. Assume  $\mathcal{S}$ , the object set of the Boolean scheme, is a collection of compact sets in  $\mathbb{R}^2$ . The centers of the Boolean scheme form a PPP of density  $\lambda$ . Then the number of blockages crossing a link  $\mathbf{OX}$  of distance  $R$  is a Poisson random variable of mean  $\lambda \mathbb{E}[V(\mathbf{OX} \oplus D)]$ , where  $D$  ranges over  $\mathcal{S}$ .*

## 3.2 Incorporating Height

In this section we extend the system model to incorporate height.

For a link  $\mathbf{OX}$  of length  $R$  in  $\mathbb{R}^2$ ,  $H_t$  is the height of the base station.  $H_r$  is the height of the mobile user. Without loss of generality, assume  $H_t > H_r$ . The heights of random blockages  $H_k$  are i.i.d. according to some probability density function  $f_H(x)$ , and independent of  $\{\mathbf{C}_k, L_k, \Theta_k\}$ . In this part, assume  $W \equiv 0$ , i.e. use line segments process to describe random buildings.

Denote  $\hat{K}$  as the number of blockages that effectively block the direct propagation of the link  $\mathbf{OX}$  when considering height of blockages. Note that even if the projection of a building on the ground cross  $\mathbf{OX}$ , in practice it might not be tall enough to actually block the link as indicated in Fig. 3.2.

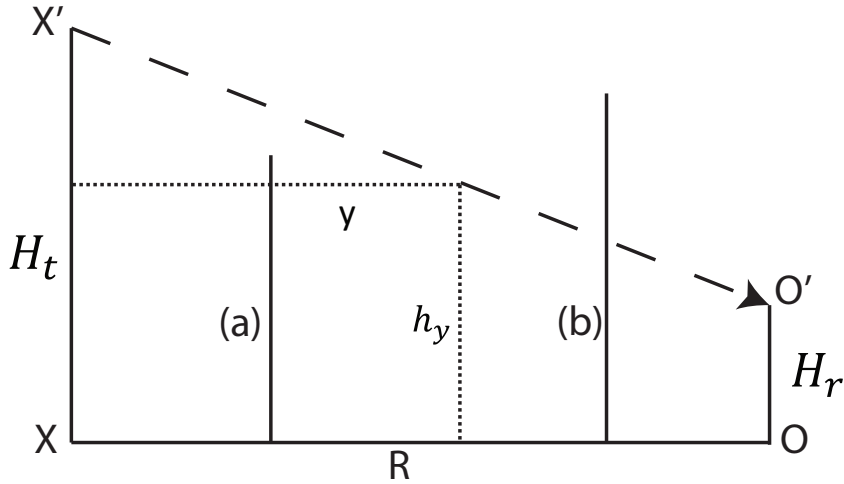


Figure 3.2: The transmitter locating at  $\mathbf{X}$  has a height of  $H_t$ , while the mobile receiver has a height of  $H_r$ . Not all buildings which cross  $\mathbf{OX}$  blockage the actual propagation path  $\mathbf{O'X'}$  in  $\mathbb{R}^3$ , such as building (a) in the figure. If a building intersecting  $\mathbf{OX}$  at a point  $y$  away from the transmitter  $\mathbf{X}$  effectively blocks  $\mathbf{O'X'}$  if only if its height is larger than  $h_y$  as building (b) in the figure.

**Theorem 3.2.1.** *Considering height,  $\hat{K}$  the number of effective blockages of*



a link of length  $R$  is a Poisson random variable with  $\mathbb{E}[\hat{K}] = \eta\mathbb{E}[K]$ , where  $\mathbb{E}[K] = \frac{2\lambda\mathbb{E}[L]R}{\pi}$ , and

$$\eta = 1 - \int_0^1 \int_0^{sH_t + (1-s)H_r} f_H(h) dh ds.$$

Note that given the distributions of heights,  $\eta$  is a constant. Moreover,  $\eta$  can be interpreted as the probability that given a building crossing  $\mathbf{OX}$ , it also blocks  $\mathbf{O'X'}$  as shown in Fig. 3.2.

*Proof.* Consider a building intersecting the link  $\mathbf{OX}$  at the point which is at a horizontal distance  $y$  away from  $\mathbf{X}$ . As shown in Fig. 3.2, the building blocks the direct propagation path  $\mathbf{O'X'}$  if only if its height  $h > h_y$ , where  $h_y$  can be computed as

$$\begin{aligned} h_y &= \frac{y(H_t - H_r)}{R} + H_r \\ &= \frac{yH_t + (R - y)H_r}{R}. \end{aligned} \quad (3.3)$$

Next given that a building intersects the link  $\mathbf{OX}$ , the intersection is uniformly distributed across the link, which indicates  $y$  is uniformly distributed on  $[0, R]$ . Hence given a building intersects  $\mathbf{OX}$ , the probability it blocks  $\mathbf{O'X'}$  is

$$\begin{aligned} \eta &= \int_0^R \int_{h_y}^{+\infty} f_H(h) \frac{1}{R} dh dy \\ &= \int_0^R \frac{1}{R} \left( 1 - \int_0^{\frac{yH_t + (R-y)H_r}{R}} f_H(h) dh \right) dy \end{aligned} \quad (3.4)$$

$$\begin{aligned} &= \int_0^1 \left( 1 - \int_0^{sH_t + (1-s)H_r} f_H(h) dh \right) ds \\ &= 1 - \int_0^1 \int_0^{sH_t + (1-s)H_r} f_H(h) dh ds, \end{aligned} \quad (3.5)$$

where (3.4) is obtained by substituting (3.3), and (3.5) is from a change of variable as  $s = \frac{y}{R}$ .

Since  $\eta$  is only determined by the distribution of the heights, which is independent of  $K$ ,  $\hat{K}$  can be viewed as the result of independent thinning of  $K$  with a parameter of  $\eta$ . Hence  $\hat{K}$  is also Poisson, and  $\mathbb{E}[\hat{K}] = \eta\mathbb{E}[K]$ .  $\square$

Although we show some extensions of results in Theorem 3.1.1, such as generalizing to the process of general shapes and incorporating height, we will restrict the discussions in the following sections to the original case where blockages are described as a rectangle Boolean scheme in  $\mathbb{R}^2$ .

### 3.3 Quantification of Power Losses by Blockages

Now armed with the distribution of the number of blockages per link, we continue to quantify the power losses due to blockages by deriving its distribution in this part. The power losses caused by random blockages on a link is expressed as  $S = \prod_{k=1}^K \gamma_k$ , where  $K$  is the number of blockages on the path, and  $\gamma_k$  is the ratio of power losses due to  $k$ -th blockage. We have already established that  $K$  is a Poisson variable with parameter  $\beta R + p$ .

If we use  $[\ ]$  to represent quantity in dB, then the ratio of penetration loss in dB is  $[S] = \sum_{k=1}^K [\gamma_k]$ , where  $[\gamma_k] = 10 \log_{10} \gamma_k$ . Since we ignore the reflections of signals,  $S$  is a nonnegative number no larger than 1. Thus  $[S]$  is always no large than 0. It is most useful to evaluate penetration loss in dB, for the statistics of penetration losses through different materials, i.e  $\gamma_k$ , are

mostly recorded in dB.

Next, we will focus on deriving the distribution of  $[S]$  with the assumption that  $[\gamma_k]$  are i.i.d. with some distribution  $f_{[\gamma_k]}(x)$ . The Laplace transform of a random variable is used to simplify the computation. For a random variable  $X$  in  $\mathbb{R}^+$ , its Laplace transform  $\mathbb{L}_X(s)$  is defined as

$$\mathbb{L}_X(s) = \mathbb{E} [e^{-sX}] = \int_0^{\infty} f_X(x)e^{-sx} dx, \quad (3.6)$$

where  $f_X(x)$  is the probability density function of  $X$ . Note that in theory, knowing the Laplace transform of  $X$  is equivalent to knowing its distribution, for the probability density function can be obtained by computing the inverse Laplace transform of  $\mathbb{L}_X(s)$ . We obtain  $\mathbb{L}_{[S]}(t)$  for general distributions of  $[\gamma_k]$  in the following theorem.

**Theorem 3.3.1.** *Assume the penetration losses of a blockage  $[\gamma_k]$  are i.i.d. in a link of length  $R$ . The Laplace transform of  $[\gamma_k]$  is  $\mathbb{L}_{[\gamma_k]}(t)$ .  $\beta$  and  $p$  are coefficients from the Boolean scheme of blockages as defined in the previous part. Then the Laplace transform of  $[S]$ , the total power losses of the link by blockages can be computed as*

$$\mathbb{L}_{[S]}(t) = e^{(\beta R + p)(\mathbb{L}_{[\gamma_k]}(t) - 1)} \quad (3.7)$$

*Proof.* Since  $[\gamma_j]$  are i.i.d., we have

$$\begin{aligned}
\mathbb{L}_{[S]}(t) &= \mathbb{E} \left[ e^{-t \sum_{k=1}^K [\gamma_k]} \right] \\
&= \mathbb{E}_K \left[ \prod_{k=1}^K \mathbb{E}_{[\gamma_k]} \left[ e^{-t[\gamma_k]} \right] \right] \\
&= \mathbb{E}_K \left[ \left[ \mathbb{L}_{[\gamma_k]}(t) \right]^K \right] \\
&\stackrel{(a)}{=} e^{(\beta R + p)(\mathbb{L}_{[\gamma_k]}(t) - 1)},
\end{aligned}$$

where (a) follows the fact that  $K$  is a Poisson variable with parameter  $\beta R + p$ .  $\square$

For generally distributed  $[\gamma_k]$ , the distribution of  $[S]$  has no closed-form expression, and can be obtained through numerical integrals. Closed form expression, however, can be obtained in certain cases as shown in the following corollaries.

**Corollary 3.3.1.1.** *If for any  $k$ ,  $[\gamma_k] \equiv [\gamma]$ , then  $\mathbb{L}_{[S]}(t) = e^{(\beta R + p)(e^{-t[\gamma]} - 1)}$ . In the impenetrable case when  $\gamma = 0$ ,  $S$  is a Bernoulli random variable with parameter as  $\mathbb{P}\{S = 1\} = e^{-(\beta R + p)}$ .*

**Corollary 3.3.1.2.** *Assume that  $\gamma_k$  is i.i.d uniformly distributed on  $[0, 1]$ . Then  $f_{[S]}(x)$  the probability density function of  $[S]$  is*

$$\begin{aligned}
f_{[S]}(x) &= e^{-(\beta R + p)} \delta(x) + e^{-(\beta R + p - 0.1 \ln 10 x)} \sqrt{\frac{-0.1 \ln 10 (\beta R + p)}{x}} \\
&\quad \times I_1 \left( 2 \sqrt{\frac{-\ln 10}{10} x (\beta R + p)} \right), \tag{3.8}
\end{aligned}$$

where  $x < 0$ ,  $\delta(x)$  is the Dirac delta function, and  $I_1$  is the first-order modified Bessel function of the first kind. The probability density function of  $S$  is

$$f_S(y) = e^{-(\beta R+p)}\delta(y-1) + e^{-(\beta R+p)}\sqrt{-\frac{\beta R+p}{\ln y}}I_1\left(2\sqrt{-(\beta R+p)\ln y}\right), \quad (3.9)$$

where  $y \in (0, 1]$ .

*Proof.* Observe that

$$\begin{aligned} \mathbb{L}_{[S]}(t) &= \mathbb{E}_K \left[ [\mathbb{L}_{[\gamma_j]}(t)]^K \right] \\ &= \sum_{n=0}^{\infty} \frac{e^{-(\beta R+p)}(\beta R+p)^n}{n!} [\mathbb{L}_{[\gamma_j]}(t)]^n \end{aligned} \quad (3.10)$$

Also note that the Laplace transform of  $[\gamma_k]$  is

$$\mathbb{L}_{[\gamma_k]}(t) = \frac{0.1 \ln 10}{0.1 \ln 10 + t} \quad (3.11)$$

Then substitute (3.11) into (3.10), and compute the inverse Laplace transform of each term in the right hand side. This leads to

$$f_{[S]}(x) = e^{-(\beta R+p)}\delta(x) + \sum_{m=0}^{\infty} \frac{e^{-(\beta R+p-0.1 \ln 10x)} [0.1 \ln 10 (\beta R+p)]^{m+1} (-x)^m}{(m)! (m+1)!},$$

which can be simplified to (3.8) by using the notation of modified Bessel function of the first kind. By changing variable as  $y = e^{0.1 \ln 10x}$  in (3.8), we obtain (3.9).  $\square$

Even if  $\gamma_k$  is a continuous random variable on  $[0, 1]$ ,  $S$  always has a discontinuity at  $x = 1$  as the form of Dirac delta function  $\delta(x-1)$ , which indicates the probability of no power losses by blockages. Hence the amplitude

of the impulse  $\delta(x - 1)$  equals the probability that a link admits line-of-sight propagation as computed in Corollary 3.1.1.1.

Since the closed-form expression for  $f_S(x)$  is generally hard to obtain through inverse Laplace transform, we consider an approximation of the continuous part of  $f_S(x)$  using the beta distribution, which has also been applied to model the behavior of random variables with support on intervals of finite length in a wide variety of disciplines [25]. We assume the target probability density function of the approximation to be

$$f_{\hat{S}_i}(x) = (1 - e^{-(\beta R+p)}) \frac{\Gamma(a+b)}{\Gamma(a)\Gamma(b)} x^{a-1} (1-x)^{b-1} + e^{-(\beta R+p)} \delta(x-1), \quad (3.12)$$

where  $\Gamma(z)$  is the gamma function defined as  $\Gamma(z) = \int_0^\infty t^{z-1} e^{-t} dt$ .

The parameters  $a$  and  $b$  in (3.12) can be determined by matching the moments of  $S$ . The moments of  $S$  can be computed through the following theorem.

**Theorem 3.3.2.** *Assume  $\gamma_j$  are i.i.d. random variable on  $[0, 1]$ . The  $n$ -th moment of  $S$  is*

$$\mathbb{E}[S^n] = e^{-(\beta R+p)(1-\mathbb{E}[\gamma_k^n])}. \quad (3.13)$$

*Proof.* The proof is straightforward as

$$\begin{aligned} \mathbb{E}[S^n] &= \mathbb{E} \left[ \prod_{k=1}^K \gamma_k^n \right] \\ &= \mathbb{E}_K \left[ (\mathbb{E}[\gamma_k^n])^K \right] \\ &\stackrel{(b)}{=} e^{-(\beta R+p)(1-\mathbb{E}[\gamma_k^n])}, \end{aligned}$$

where (b) comes from computing the moment generating function of  $K$ , which is a Poisson random variable.  $\square$

The values of  $a$  and  $b$  in (3.12) can be computed through one direct corollary as follows.

**Corollary 3.3.2.1.** *Matching the first and second moment of  $S$ ,  $a$  and  $b$  in (3.12) can be obtained by solving*

$$\begin{cases} \frac{a(1-e^{-(\beta R+p)})}{a+b} + e^{-(\beta R+p)} = e^{-(\beta R+p)(1-\mathbb{E}[\gamma_k])}, \\ \frac{a(a+1)(1-e^{-(\beta R+p)})}{(a+b)(a+b+1)} + e^{-(\beta R+p)} = e^{-(\beta R+p)(1-\mathbb{E}[\gamma_k^2])}. \end{cases} \quad (3.14)$$

### 3.4 Analysis of Blockage Effects on Link Budget

In this section, we investigate the blockage effects on link budget by deriving new path loss formulae which account for the penetration losses on a link. By Theorem 3.3.2, we derive the following formula.

**Corollary 3.4.0.2.** *Considering the blockages in a network, the average received power  $\mathbb{E}[P_r]$  on a link of distance  $R$  is*

$$\mathbb{E}[P_r] = \frac{C\mathbb{E}[g]\mathbb{E}[S]}{R^\alpha} = \frac{C e^{-(\beta R+p)(1-\mathbb{E}[\gamma_k])}}{R^\alpha}, \quad (3.15)$$

where  $g$  is the small-scale fading variable with mean 1, and  $C$  is a constant determined by the signal frequency, antenna gain, and the transmitted power  $P_t$ .

Corollary 3.4.0.2 indicates that blockage effects, on average, introduce an additional exponential decay in the link budget. This observation matches

prior results in [16], where data from field experiments was used to verify the statement. Note that Corollary 3.4.0.2 provides a path loss formula for a general case, where the locations of the transmitter and receiver, whether indoor or outdoor, are not specified. We will provide the path loss formulae in both outdoor-outdoor and indoor-outdoor links in the following theorem.

**Theorem 3.4.1.** *The path loss formula for outdoor-outdoor links is*

$$\mathbb{E}[P_r] = \frac{C e^{-(\beta R - p)(1 - \mathbb{E}[\gamma_k])}}{R^\alpha}, \quad (3.16)$$

and the path loss for indoor-outdoor links is

$$\mathbb{E}[P_r] = \frac{C (1 - e^{-\mathbb{E}[\gamma_k]p}) e^{-\beta R(1 - \mathbb{E}[\gamma_k])}}{R^\alpha (1 - e^{-p})} \quad (3.17)$$

$$\stackrel{(c)}{\approx} \frac{C \mathbb{E}[\gamma_k] e^{-\beta R(1 - \mathbb{E}[\gamma_k])}}{R^\alpha}. \quad (3.18)$$

*Proof.* If the link  $\mathbf{OX}$  is an outdoor-outdoor link, then both the transmitter  $\mathbf{X}$  and the receiver  $\mathbf{O}$  are not covered by blockages. By Theorem 3.1.2, given that both  $\mathbf{O}$  and  $\mathbf{X}$  are not covered, the number of blockages is a Poisson variable with parameter  $\mathbb{E}[V(\mathbf{OX} \oplus D) - 2V(D)] = \beta R - p$ , where  $D$  ranges over the object set of the Boolean scheme of blockages. Hence, given  $\mathbf{O}$  and  $\mathbf{X}$  are not covered,  $\mathbb{E}[S] = e^{-(\beta R - p)(1 - \mathbb{E}[\gamma_k])}$ , which leads to (3.16) directly.

Similarly, for the indoor-outdoor link, conditioning on that exactly one of  $\mathbf{X}$  and  $\mathbf{O}$  is covered by blockages,  $\mathbb{E}[S] = \frac{(1 - e^{-\mathbb{E}[\gamma_k]p}) e^{-\beta R(1 - \mathbb{E}[\gamma_k])}}{1 - e^{-p}}$ , which leads to (3.17). The approximation in (c) follows from the fact that  $\lim_{p \rightarrow 0} \frac{1 - e^{-\mathbb{E}[\gamma_k]p}}{1 - e^{-p}} = \mathbb{E}[\gamma_k]$   $\square$



*Remark 3.4.1.* By Theorem 3.4.1, in a cellular network an indoor user will, on average, receive signals  $e^{-p(1-\mathbb{E}[\gamma_k])}\mathbb{E}[\gamma_k] \approx \mathbb{E}[\gamma_k]$  weaker than an outdoor user does. This motivates the wide deployment of femtocells.

## Chapter 4

# Analysis of Blockage effects on Impenetrable Networks

In the previous chapter, we derived the distribution of power losses caused by blockages, and analyzed blockage effects on point-to-point links. In this chapter, we apply these results to analyze the effects of blockages on the performance of cellular networks. Before we consider the general case, we first study an impenetrable network where  $\gamma_{ik} = 0$  such that the signals are totally absorbed by the blockages.

To maintain the tractability of analysis, we make one key approximation: blockages affect each link independently. Strictly speaking, the number of blockages on different links are not always independent. For instance, if two base stations happen to locate on the same ray originating from the mobile user, then the base station further from the user will always have no fewer buildings on the link than the closer one has. Thus these two links are correlated. There are cases, however, where the number of the blockages on the two links are independent. For example, whenever two links share no common blockages, the numbers of blockages on the links are independent. Though an approximation, the assumption of link independence is acceptable when the

sizes of blockages  $L_i$  and  $W_i$  are relatively small compared with the distances of links  $\mathbf{OX}_i$ . Moreover, it provides us much tractability to analyze networks with independent links. Discussion on the correlation of shadowing among links can be found in [26, 27]

## 4.1 Connectivity

In a cellular network with impenetrable blockages, blockages would limit the communication range of a base station. Intuitively, blockages divide the plane into many isolated “islands”. Only the locations with the same “island” can communicate directly via wireless links. Thus in this section, we investigate the connectivity of an impenetrable networks. Specifically, we aim to answer the following questions: (i) How many candidate base stations, i.e. the unblocked base stations, are there for a typical user? (ii) What is the distance to the nearest candidate base station?

Related results have been investigated in mathematics, and can be found under the topics of vacancy [19] and contact distance [28]. We will use the methodology proposed in [17] in this section.

To begin with, we introduce the following notation. With some abuse of the notation  $K_i$ , for  $\mathbf{x}, \mathbf{y} \in \mathbb{R}^2$ , we define  $K_{xy}$  as the number of blockages on the direct link connecting  $\mathbf{x}$  and  $\mathbf{y}$ . Further, we define the concept of *visible area* in the impenetrable networks as below.

**Definition 4.1.1.** For any  $\mathbf{x}, \mathbf{y}$  in  $\mathbb{R}^2$ ,  $\mathbf{x}$  is *visible* by  $y$  if and only if  $K_{xy} = 0$ ,

i.e. no blockage intersects the link  $\mathbf{x}\mathbf{y}$ . Moreover, if  $\mathbf{x}$  is not contained by a blockage, define  $Q_x$  the visible region of  $\mathbf{x}$  as the set of all points on  $\mathbb{R}^2$  visible by  $\mathbf{x}$ . Namely, if  $\mathbf{x}$  does not locate inside a blockage,

$$Q_x = \{\mathbf{y} \in \mathbb{R}^2 : K_{xy} = 0\}. \quad (4.1)$$

If  $x$  is inside a building, we consider it has no visible area, i.e.  $Q_x = \phi$ .

Note that in a impenetrable network a mobile user at  $\mathbf{x}$  can only connect to base stations located in its visible area  $Q(x)$ . The average size of visible area can be computed through the following theorem.

**Theorem 4.1.1.** *In cellular networks with impenetrable blockages,  $\forall \mathbf{x} \in \mathbb{R}^2$ , the average size of the visible region of  $\mathbf{x}$  is*

$$\mathbb{E}[V(Q_x)] = \frac{2\pi e^{-p}}{\beta^2}. \quad (4.2)$$

*Proof.* Since the blockages are modelled as a Boolean scheme of rectangles, which is stationary in  $\mathbb{R}^2$ , it is sufficient to check the visible area of the origin  $Q_0$ . Denote  $A$  as the event that the origin is not covered by a blockage. By Corollary 3.1.1.2,

$$\mathbb{P}\{A\} = e^{-p}.$$

If  $A$  is not true, then  $Q_0 = 0$ . Thus we focus on the case when the origin is not inside any blockage in the following part of proof.

Define  $\{\mathbf{a}_\psi\}$  as the set of normalized vectors, where  $\psi$  is the angle between  $\mathbf{u}_\psi$  and  $x$  axis. Define  $D(\psi)$  as

$$D(\psi) = \sup\{r \in \mathbb{R}^+ : K_{r\mathbf{u}_\psi} = 0\}. \quad (4.3)$$

Namely,  $D(\psi)$  is the distance to the nearest blockage along the direction  $\mathbf{u}_\psi$ .

Next we show that conditioning on  $A$ ,  $D(\psi)$  is an exponential random variable with parameter  $\beta$ . By Corollary 3.1.1.1,

$$\begin{aligned} \mathbb{P}\{D(\psi) > R|A\} &= \frac{\mathbb{P}\{K_{R\mathbf{u}_\psi} = 0\}}{\mathbb{P}\{A\}} \\ &= \frac{e^{-(\beta R+p)}}{e^{-p}} \\ &= e^{-\beta R} \end{aligned}$$

Hence using polar coordinate, the total average size of the visible area conditioning on  $A$  is

$$\begin{aligned} \mathbb{E}[V(Q_0)|A] &= \int_0^{2\pi} \frac{\mathbb{E}[D^2(\psi)]}{2} d\psi \\ &= \int_0^{2\pi} \int_0^\infty \frac{r^2}{2} d\psi \beta e^{-\beta r} dr \\ &= \frac{2\pi}{\beta}. \end{aligned}$$

Finally, the average size of the visible area is

$$\begin{aligned} \mathbb{E}[V(Q_0)] &= \mathbb{P}\{A\}\mathbb{E}[V(Q_0)|A] + (1 - \mathbb{P}\{A\}) \times 0 \\ &= \frac{2\pi e^{-p}}{\beta^2}. \end{aligned}$$

□

We define the *effective visible range* of a network  $R_{eff}$  as the radius of a circle whose area equals the average visible area  $\mathbb{E}[V(Q_0)]$  of the network. It directly follows from Theorem that

$$R_{eff} = \left( \sqrt{\frac{\mathbb{E}[V(Q_0)]}{\pi}} \right) = \frac{\sqrt{2e^{-p}}}{\beta}. \quad (4.4)$$

Note that  $R_{eff}$  can reveal the average range that a base station can reach via line-of-sight links in a network.

The average number of visible base stations to a mobile user is also derived in the following corollary.

**Corollary 4.1.1.1.** *In cellular networks with impenetrable blockages, if the base stations form a homogeneous PPP with density  $\mu$ , the average number of visible base stations to a mobile user is  $\mu\mathbb{E}[V(Q_0)] = \frac{2\pi\mu e^{-p}}{\beta^2}$ .*

*Proof.* By Theorem 4.1, the size of the visible area is finite almost surely, for the average size of the visible area is finite. Thus we denote the probability density function of the visible area as  $f_V(v)$ .

For a realization of blockages, the mobile user has a finite visible area of size  $v$ . By Assumption 2.2.1, the PPP of base stations is independent of the Boolean scheme of blockages. Hence for this realization of blockages, the mobile user has  $\mu v$  visible base stations on average. Averaging all the realizations of blockages, we have the average number of visible base stations as

$$\int_0^\infty \mu v f_V(v) dv = \mu\mathbb{E}[V(Q_0)].$$

□

Next we derive the distribution of the distance to the closest visible base stations under the assumption that the number of blockages on each link is independent.

**Theorem 4.1.2.** *Assuming the numbers of blockages on all links are independent, then the distribution of the distance to the closest visible base station  $R_0$  is*

$$\mathbb{P}\{R_0 > x\} = \exp(-2\pi\mu U(x)), \quad (4.5)$$

where  $U(x) = \frac{e^{-p}}{\beta^2} [1 - (\beta x + 1)e^{-\beta x}]$ .

*Proof.* Assume that the mobile user is located at the origin. The distance to the nearest visible BS  $R_0$  is larger than  $x$  if only if all the base stations located within the ball  $\mathcal{B}(\mathbf{O}, x)$ , if there is any, are not visible to the user. Since the base stations form a PPP of density  $\mu$ , it follows that

$$\begin{aligned} \mathbb{P}\{R_0 > x\} &= \mathbb{P}\{\text{all base stations in } \mathcal{B}(\mathbf{O}, x) \text{ are not visible}\} \\ &= \sum_{i=0}^{\infty} \left[ \int_0^x (1 - e^{-(\beta t + p)}) \frac{2t}{x^2} dt \right]^i \frac{e^{-\mu\pi x^2} (\mu\pi x^2)^i}{i!} \\ &= \sum_{i=0}^{\infty} \left( 1 - \frac{2U(x)}{x^2} \right)^i \frac{e^{-\mu\pi x^2} (\mu\pi x^2)^i}{i!} \\ &= e^{-\mu\pi x^2 [1 - (1 - \frac{2U(x)}{x^2})]} \\ &= e^{-2\mu\pi U(x)}. \end{aligned}$$

□

One direct corollary of Theorem 4.1.2 follows by differentiating (4.5).

**Corollary 4.1.2.1.** *The probability density function of  $R_0$  is*

$$f_{R_0}(x) = 2\pi\mu x e^{-(\beta x + p + 2\pi\mu U(x))}.$$

In a network with impenetrable blockages, a mobile user can be only served by the base stations in his visible area. If there happens to be no base stations located inside the visible region, the mobile user will have no chance to be covered. We define the *silent* area of an impenetrable network as the set of all locations which have no visible base stations. Next we estimate the ratio of silent area  $\rho$  in a cellular network.

**Corollary 4.1.2.2.** *Under the independent link assumption, the ratio of the silent area  $\rho$  in a network with impenetrable blockages is*

$$\rho = 1 - \mathbb{P}(R_0 < \infty) = \exp\left(-\frac{2\mu\pi e^{-p}}{\beta^2}\right). \quad (4.6)$$

*Proof.* Since the distribution of the base stations and blockages are stationary on the plane, the ratio of the silent area equals the probability that any location in  $\mathbb{R}^2$ , for example the origin, has no visible base stations, which also equals the probability that the closest visible base station of the origin is infinitely far away, i.e  $1 - \mathbb{P}(R_0 < \infty)$ . Hence, it follows

$$\begin{aligned} 1 - \mathbb{P}\{R_0 < \infty\} &= \lim_{x \rightarrow \infty} \mathbb{P}\{R_0 > x\} \\ &= \exp\left[-2\mu\pi e^{-p} \lim_{x \rightarrow \infty} \left(\frac{1}{\beta^2} (1 - e^{-\beta x(1+x)})\right)\right] \\ &= \exp\left(\frac{-2\mu\pi e^{-p}}{\beta^2}\right). \end{aligned}$$



□

*Remark 4.1.1.* Note that  $\rho$  illustrates the level of connectivity in a network. When  $\rho$  increases, mobile users become less likely to get connected in the network. Considering  $\beta = \frac{2\lambda(\mathbb{E}[L]+\mathbb{E}[W])}{\pi}$  for (4.6), the ratio of silent area is

$$\rho = 1 - \exp\left(\frac{-\pi^3\mu}{2\lambda^2 e^{-\lambda\mathbb{E}[W]\mathbb{E}[L]} (\mathbb{E}[L] + \mathbb{E}[W])^2}\right).$$

This indicates that to keep the connectivity fixed, the density  $\mu$  of base stations should scale superlinearly with the blockage density  $\lambda$ . Specifically when  $p$  is small,  $\mu$  should scale with  $\lambda^2$  approximately.

## 4.2 Coverage Probability

The coverage probability is one of the most important performance metric in cellular networks. In a interference-limited network, coverage probability is defined as

$$P_c(T) = \mathbb{P}\{\text{SIR} > T\}, \quad (4.7)$$

where  $T > 0$  is the SIR threshold for successful decoding at the receiver. The coverage probability can be also interpreted as the average percentage of area within a cell that has received power above a given threshold.

Note that though not expressed explicitly,  $P_c(T)$  can also be a function of base station density  $\mu$ , blockage density  $\lambda$ , and other statistics of blockages, such as  $\mathbb{E}[L]$  and  $\mathbb{E}[W]$ . More importantly,  $P_c$  also depends on the connecting strategy of the user. For instance, a mobile user can connect to the base

station that provides maximum SIR or the strongest signal power. For the tractability of the analysis, we assume the mobile user always connects to the *nearest* visible base station if there is any visible base station.

The number of blockages on each link is generally not independent in a network. Hence the correlation between links in terms of blockage effects renders the performance metrics in an impenetrable network hard to express in analytical forms. To obtain an analytical approximation of the coverage probability, we therefore ignore the correlation between links, and assume that each link is independent in terms of blockage numbers. In this case, the coverage probability can be approximated through the following theorem. We will show in Chapter 5, that this method provides a relatively tight approximation of  $P_c(T)$  by simulations.

**Theorem 4.2.1.** *If the user connects to the nearest visible base station, the coverage probability  $P_c(T)$  can be approximated by*

$$P_c(T) \approx \int_{0^+}^{\infty} \exp\left(-2\pi\mu \int_x^{\infty} \left[\frac{Tx^\alpha e^{-(\beta t+p)}}{t^\alpha + Tx^\alpha}\right] t dt\right) f_{R_0}(x) dx, \quad (4.8)$$

where  $f_{R_0}(x)$  is the probability density function of the distance to the nearest visible base station derived in Corollary 4.1.2.1,  $\alpha$  is the path loss exponent as in (2.2).

*Proof.* First we compute the expression of coverage probability conditioning on the distance to the nearest visible base station  $R_0$ . Given that  $R_0 = x$ , the

expression of SIR is

$$\text{SIR} = \frac{x^{-\alpha} g_0}{\sum_{i:R_i>x} R_i^{-\alpha} g_i S_i},$$

where  $g_i$  are i.i.d. exponential random variables with mean 1,  $S_i$  in the impenetrable case are Bernoulli random variables with parameter  $e^{-(\beta R_i+p)}$ . If we ignore the correlation of the number of blockages between links, then  $S_i$  are independent. The conditional coverage probability follows as

$$\begin{aligned} \mathbb{P}\{\text{SIR} > T | R_0 = x\} &= \mathbb{P}\{h_0 > T x^\alpha \sum_{i:R_i>x} R_i^{-\alpha} g_i S_i\} \\ &= \mathbb{E} \left[ \exp \left( -T x^\alpha \sum_{i:R_i>x} R_i^{-\alpha} g_i S_i \right) \right] \\ &\stackrel{(d)}{\approx} \mathbb{E} \left[ \prod_{i:R_i>x} \mathbb{E}_{S_i, g_i} [\exp(-T x^\alpha R_i^{-\alpha} g_i S_i)] \right] \\ &= \mathbb{E} \left( \prod_{i:R_i>x} \mathbb{E}_{g_i} [\exp(-T x^\alpha g_i R_i^{-\alpha})] e^{-(\beta R_i+p)} + 1 - e^{-(\beta R_i+p)} \right) \\ &= \mathbb{E} \left( \prod_{i:R_i>x} 1 - \frac{T x^\alpha e^{-(\beta R_i+p)}}{R_i^\alpha + T x^\alpha} \right) \\ &\stackrel{(e)}{=} \exp \left( -2\pi\mu \int_x^\infty \left[ \frac{T x^\alpha e^{-(\beta t+p)}}{t^\alpha + T x^\alpha} \right] t dt \right), \end{aligned}$$

where the approximation in (d) is from the assumption to ignore the correlation between links, and (e) follows directly from computing Laplace functional of the PPP formed by the base stations  $\{X_i\}$  [24]. The unconditional coverage

probability follows as

$$\begin{aligned}
P_c(T) &= \mathbb{P}(\text{SIR} > T) \\
&= \int_{x>0} \mathbb{P}(\text{SIR} > T | R_0 = x) f_{R_0}(x) dx \\
&\approx \int_{0^+}^{\infty} \exp\left(-2\pi\mu \int_x^{\infty} \left[\frac{T x^\alpha e^{-(\beta t+p)}}{t^\alpha + T x^\alpha}\right] t dt\right) f_{R_0}(x) dx.
\end{aligned}$$

□

*Remark 4.2.1.* Note that by (4.8), considering blockage effects, the coverage probability in a interference-limited network is not invariant with base station density.

### 4.3 Average Achievable Rate

We investigate another important performance metric, the average achievable rate in this part. The average achievable rate  $\tau$  is defined as

$$\tau = \mathbb{E}[\log_2(1 + \text{SIR})]. \quad (4.9)$$

**Theorem 4.3.1.** *Given the coverage probability  $P_c(T)$  in a cellular network with impenetrable blockages, the average achievable rate  $\tau$  is*

$$\tau = \frac{1}{\ln 2} \int_{T>0} \frac{P_c(T)}{T+1} dT. \quad (4.10)$$

*Proof.* See [5].

□

If we apply the approximation of coverage probability  $P_c(T)$  in Theorem 4.2.1 to (4.10), then we obtain an approximation of the achievable rate in an impenetrable network.

Note that it is possible that there is exactly one base station located in the visible area of a mobile user, though the possibility is small. In this case, the mobile user will receive no interference but only desired signal, which renders the SIR infinite. Hence, even taking thermal noise into account, the convergence of (4.10) is very slow if it converges. In reality, the SINR will never be infinitely large, for thermal noise, and more importantly, the nonlinear distortion [29] at the receiver will limit the actual received SINR. For instance, even ignoring interference, the typical signal-to-noise and distortion ratio alone for VHF and UHF radio is 12dB. Hence, at this stage, we assume the operating SIR is upper bounded by a threshold  $M$ . Namely, given that  $R_0 = x$ , the operating SIR is

$$\text{SIR} = \min \left\{ \frac{x^{-\alpha} g_0}{\sum_{i:R_i>x} R_i^{-\alpha} g_i S_i}, M \right\}. \quad (4.11)$$

Finally, with the refined SIR expression in (4.11), the average rate can be evaluated as

$$\tau \approx \frac{1}{\ln 2} \int_0^M \frac{P_c(T)}{T+1} dT. \quad (4.12)$$

# Chapter 5

## Simulation Results

In this chapter, we present some simulation results to compare our proposed model with prior work, and illustrate how blockage effects impact the network performance.

First, we compare the simulation results based on the proposed Boolean scheme model and the lattice model in [13]. The original lattice model proposed in [13] assumes a random lattice of unit squares, each of which is occupied by a blockage with some probability. To make a fair comparison, we extend the model to a lattice made up of rectangle sites of size  $\mathbb{E}[L] \times \mathbb{E}[W]$ . Each site is occupied by a blockage with probability  $p$ , where  $\mathbb{E}[L]$ ,  $\mathbb{E}[W]$  and  $p$  are parameters in the proposed Boolean scheme model, such that the average number of blockages on a link is the same in both the Boolean scheme model and the lattice model.

Fig. 5.1 shows that the comparison of simulated SIR distributions in both models with equivalent parameters. Though the average number of blockages in each link is identical, SIR distributions are different due to the fact that the Boolean scheme model allows the blockage orientation and size to be random. Hence we conclude that it is important to incorporate the

randomness of orientation and size in the blockage model, which is not fully investigated in the prior work.

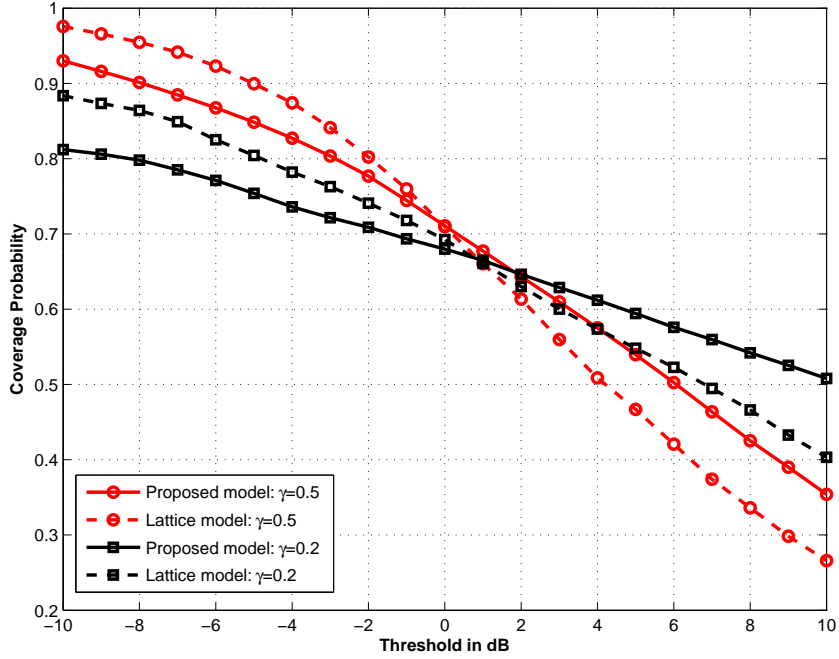


Figure 5.1: We compare the proposed Boolean scheme model with the lattice model. All curves are drawn according to Monte Carlo simulations, where  $p = 0.3$ ,  $\mathbb{E}[L] = \mathbb{E}[W] = 15$  meters. The ratio of penetration loss per building  $\gamma$  is assumed to be constant. In the Boolean scheme model, we assume the lengths and widths of the blockages are i.i.d. uniformly distributed. Difference in the SIR distributions is observed when using different blockage models, which indicates that the distributions of the blockage orientation and size affect the network performance.

Next, we consider the blockage effects on cellular networks with impenetrable blockages. Simulations of the network connectivity are illustrated in Fig. 5.2 as a function of the density and size of the blockages. Both the average visible area and the ratio of silent area are examined in the simulations.

Results in Fig. 5.2 indicate that the existence of blockages will limit the range of line-of-sight links, and increase the ratio of silent areas in a network.

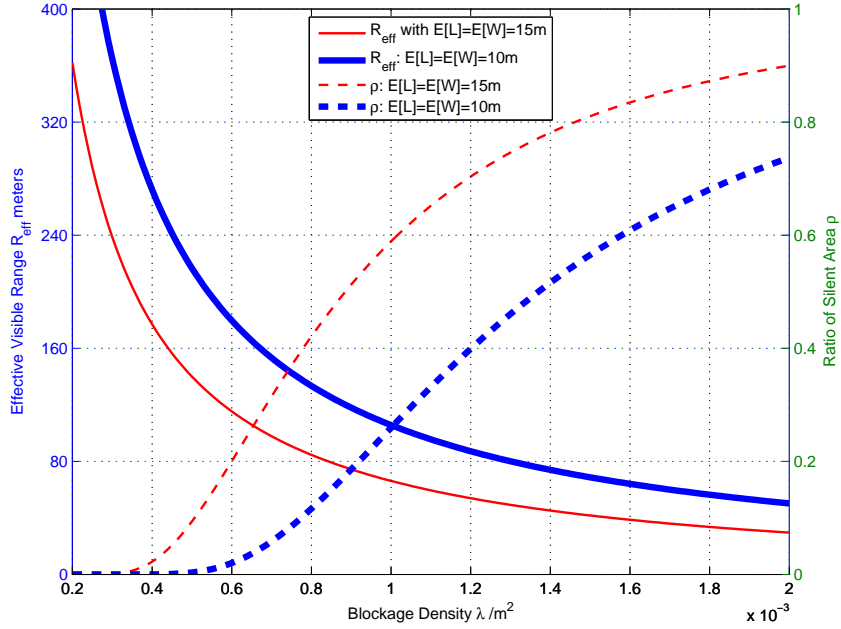


Figure 5.2: The network connectivity is examined in terms of the average visible area and the ratio of uncovered area. The density of base station is  $\mu_0 = 3.85 \times 10^{-5}$ , where the average cell radius is 100 meters. When the density and the size of blockages increase, the visible area shrinks as the ratio of silent area increases.

Fig. 5.3 presents the comparison between Monte Carlo simulations and the analytical results we derived in Section 4 in terms of coverage probability. The minor error between the curves are caused by neglecting correlations of blockage effects on different links in the analysis. Though as an approximation with some error, the analytical expression is still useful, for it takes more than 2 hours to run a Monte Carlo simulation of 10000 samples, and less than 1



minute to evaluate the coverage using the analytical expression.

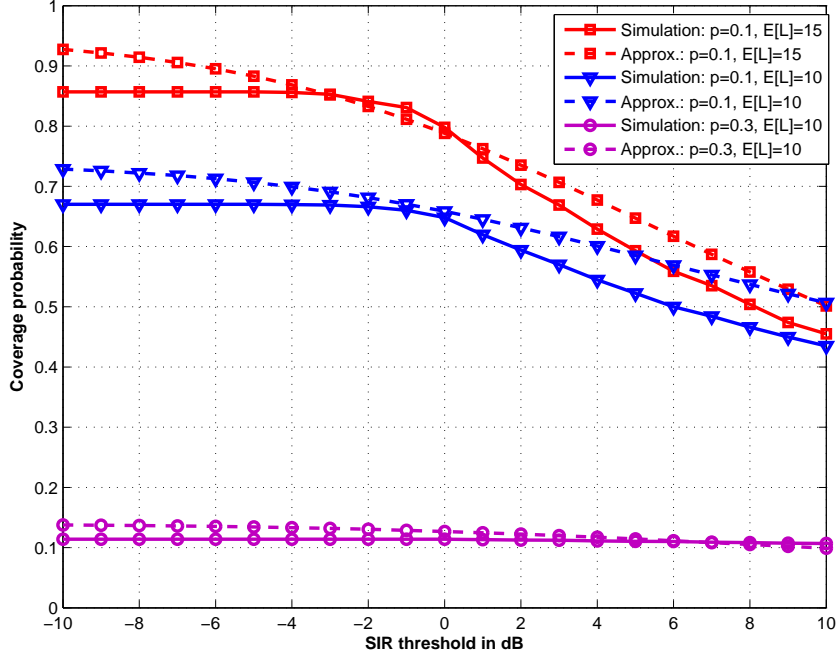


Figure 5.3: Analytic results for coverage probability is compared with Monte Carlo simulations in the impenetrable network. We assume  $W_i$  and  $L_i$  are i.i.d. uniformly distributed in the simulations. The error becomes negligible especially in the SIR regime between -5dB and 5dB.

Given a fixed blockage density, Fig. 5.4 shows that how the coverage probability change with the base stations density. Without taking the blockages into accounts, in [5] it was concluded that the coverage probability is invariant with the base station density. However, as Fig. 5.4 illustrates, with blockages, system performance in terms of SIR distribution is dependent on the base station density. Compared with the baseline curve of no blockage, we find that blockages often help improve coverage. This apparently counter-

Table 5.1: Average Rate Comparison With  $M = 10dB$ 

Base Station Density	No blockages	$0.1\mu_0$	$\mu_0$	$10\mu_0$
Average Rate (nats/sec/Hz)	1.10	0.61	1.68	1.22

intuitive result can be explained by the distance-dependent feature of blockage effects. Since we assume the user always connects to the nearest available base station, the interference link is always longer than the desired-signal link. Thus there will be more blockages on the interference links. Then a large portion of interference power will be blocked from the mobile user than that of the signal power. Furthermore, by comparing the curves of  $\mu_0$  and  $10\mu_0$ , we conclude that increasing base station density need not provide better coverage probability. Instead, increasing the number of base stations deployed in a region, as Fig. 5.4 suggests, sometimes leads to a degradation of performance. Hence with a fixed blockage density, the optimum base station density to achieve best network performance is finite. Another interesting observation is that when the base station density goes to infinity, the coverage probability converges to the case with no blockages. It can be explained as since the locations of base stations and buildings form two independent homogeneous PPPs, increasing base station density to infinity with a fixed blockage density is equivalent to decreasing the blockages density to zero with some base station density. Simulation results of the average rate provide similar insight that, considering blockage effects, the average rate is no longer invariant with base station density, and that blockages may help increase the achievable rate, as shown in Table 5.1.

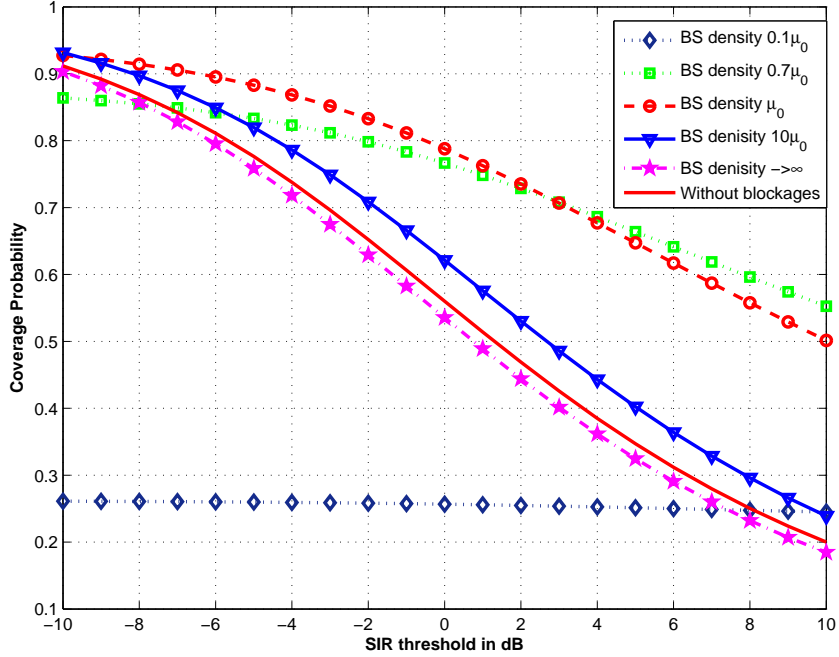


Figure 5.4: Coverage probabilities are computed through the analytical expression with different base station density, where  $\mu_0 = 3.85 \times 10^{-5}$ . Given the distribution of blockages, the coverage probability is a function of the base station density. The baseline curve with no blockages is derived according to [5]. Compared with the baseline curve, when base station density is  $\mu_0$ , a remarkable performance gain due to blockages is observed in terms of the coverage probability, which indicates blockages sometimes help to improve performance of urban networks.

## Chapter 6

### Conclusion

In this paper, we propose a stochastic framework to model random blockages in urban cellular networks using the concepts from random shape theory. The key idea is to model the random buildings as a Boolean scheme of rectangles, which allows a comprehensive characterization of the randomness of the blockages, such as sizes, locations, orientations, and heights. Based on the blockage model, we derive the distribution of the power losses due to blockages in a link, which captures the distance-dependent feature of the blockage effects. Analysis of the performance in cellular networks with impenetrable blockages indicates that blockages do change the behavior of cellular networks in a important way, such as removing the invariance with base station density in terms of SIR distribution. Most importantly, our results also illustrate the fact that cellular networks often benefit from blockages, for blockages are expected to block more interference power than signal power. The proposed framework can be extended to predict the coverage of millimeter-wave cellular networks, whose performance is susceptible to the existence of blockages. The model is expected to provide better evaluation of the performance of heterogeneous networks in urban areas, since distributed antennas and relays will be most helpful in the shadowed areas blocked by dense buildings. In addition,

future work is needed to refine the model by incorporating the reflection of signals.

## Bibliography

- [1] Z. Pi and F. Khan, “An introduction to millimeter-wave mobile broadband systems,” *IEEE Communications Magazine*, vol. 49, no. 6, pp. 101–107, Jun. 2011.
- [2] C. Anderson and T. Rappaport, “In-building wideband partition loss measurements at 2.5 and 60 GHz,” *IEEE Trans. Wireless Commun.*, vol. 3, no. 3, pp. 922 – 928, May 2004.
- [3] A. Goldsmith, *Wireless Communications*. Cambridge University Press, 2005.
- [4] A. Ghosh, N. Mangalvedhe, R. Ratasuk, B. Mondal, M. Cudak, E. Visotsky, T. Thomas, J. Andrews, P. Xia, H.-S. Jo, H. Dhillon, and T. Novlan, “Heterogeneous cellular networks: From theory to practice,” *IEEE Communications Magazine*, vol. 50, no. 6, pp. 54–64, Jun. 2012.
- [5] J. G. Andrews, F. Baccelli, and R. K. Ganti, “A tractable approach to coverage and rate in cellular networks,” *IEEE Trans. Commun.*, vol. 59, no. 11, pp. 3122–3134, Nov. 2011.
- [6] T. Brown, “Cellular performance bounds via shotgun cellular systems,” *IEEE J. Sel. Areas Commun.*, vol. 18, no. 11, pp. 2443 –2455, Nov. 2000.

- [7] M. Haenggi, J. Andrews, F. Baccelli, O. Dousse, and M. Franceschetti, “Stochastic geometry and random graphs for the analysis and design of wireless networks,” *IEEE J. Sel. Areas Commun.*, vol. 27, no. 7, pp. 1029–1046, Sept. 2009.
- [8] S. Mukherjee, “Distribution of downlink sinr in heterogeneous cellular networks,” *IEEE J. Sel. Areas Commun.*, vol. 30, no. 3, pp. 575–585, Apr. 2012.
- [9] R. W. Heath Jr., M. Kountouris, and T. Bai, “Modeling heterogeneous network interference with using poisson point processes,” *To appear in IEEE Trans. Signal Processing*, April 2013. [Online]. Available: <http://arxiv.org/abs/1207.2041>
- [10] H. S. Dhillon, R. K. Ganti, F. Baccelli, and J. G. Andrews, “Modeling and analysis of K-tier downlink heterogeneous cellular networks,” *IEEE Journal on Selected Areas in Communications*, vol. 30, no. 3, pp. 550–560, April 2012.
- [11] K. Rizk, J.-F. Wagen, and F. Gardiol, “Two-dimensional ray-tracing modeling for propagation prediction in microcellular environments,” *IEEE Transactions on Vehicular Technology*, vol. 46, no. 2, pp. 508–518, May 1997.
- [12] K. Schaubach, N. Davis, and T. Rappaport, “A ray tracing method for predicting path loss and delay spread in microcellular environments,”

- Proc. of IEEE Vehicular Technology Conference (VTC)*, vol. 2, May 1992, pp. 932–935.
- [13] G. Franceschetti, S. Marano, and F. Palmieri, “Propagation without wave equation toward an urban area model,” *IEEE Transactions on Antennas and Propagation*, vol. 47, no. 9, pp. 1393–1404, Sept. 1999.
- [14] S. Marano, F. Palmieri, and G. Franceschetti, “Statistical characterization of ray propagation in a random lattice,” *J. Opt. Soc. Am. A*, vol. 16, pp. 2459–2464, 1999.
- [15] S. Marano and M. Franceschetti, “Ray propagation in a random lattice: a maximum entropy, anomalous diffusion process,” *IEEE Transactions on Antennas and Propagation*, vol. 53, no. 6, pp. 1888–1896, Jun. 2005.
- [16] M. Franceschetti, J. Bruck, and L. Schulman, “A random walk model of wave propagation,” *IEEE Transactions on Antennas and Propagation*, vol. 52, no. 5, pp. 1304–1317, May 2004.
- [17] R. Schneider and W. Weil, *Stochastic and Integral Geometry*. Springer, 2000.
- [18] G. Matheron, *Random Sets and Integral Geometry*. Wiley, 1975.
- [19] P. Hall, *Introduction to the Theory of Coverage Processes*. Wiley, 1988.
- [20] F. Baccelli and B. Blaszczyzyn, *Stochastic geometry and wireless networks. Volume II: applications*. NOW publishers, 2009.



- [21] T. Bai, R. Vaze, and R. W. Heath Jr., “Using random shape theory to model blockage in random cellular networks,” in *Proc. of Int. Conf. on Signal Processing and Communications (SPCOM)*, Jul. 2012, pp. 1–5.
- [22] R. Cowan, “Objects arranged randomly in space: An accessible theory,” *Advances in Applied Probability*, vol. 21, no. 3, pp. 543–569, 1989. [Online]. Available: <http://www.jstor.org/stable/1427635>
- [23] D. Stoyan, W. Kendall, and J. Mecke, *Stochastic Geometry and Its Applications*. John Wiley and Sons, Ltd., 1995.
- [24] F. Baccelli and B. Blaszczyzyn, *Stochastic geometry and wireless networks. Volume I: theory*. NOW publishers, 2009.
- [25] N. Johnson, S. Kotz, and N. Balakrishnan, *Continuous Univariate Distributions*. Wiley & Sons, 1995.
- [26] C. Oestges, “Multi-link propagation modeling for beyond next generation wireless,” in *Proc. of Antennas and Propagation Conference (LAPC), 2011 Loughborough*, Nov. 2011, pp. 1–8.
- [27] N. Patwari and P. Agrawal, “Nesh: A joint shadowing model for links in a multi-hop network,” in *Proc. of IEEE Int. Conf. Acoustics Speech Signal Processing*, Apr. 2008, pp. 2873–2876.
- [28] J. Serra, *Image Analysis and Mathematical Morphology*. Academic Press, 1982.

- [29] R. Sadr, M. Shahshahani, and W. Hurd, "Degradation of signal-to-noise ratio due to amplitude distortion," *IEEE Transactions on Information Theory*, vol. 35, no. 4, pp. 874–878, Jul. 1989.

## Vita

Tianyang Bai is a graduate student at The University of Texas at Austin. He completed his B.Eng. in Communication Engineering from the Harbin Institute of Technology (HIT, class of 2011), ranking first in the Honors School. His research interests include stochastic geometry and wireless communication.

Permanent address: 3500 Greystone Drive  
Austin, Texas 78731

This thesis was typeset with L<sup>A</sup>T<sub>E</sub>X<sup>†</sup> by the author.

---

<sup>†</sup>L<sup>A</sup>T<sub>E</sub>X is a document preparation system developed by Leslie Lamport as a special version of Donald Knuth's T<sub>E</sub>X Program.